Environmental Science
Processes & Impacts

Accepted Manuscript

ROYAL SOCIETY OF CHEMISTRY

rsc.li/process-impacts

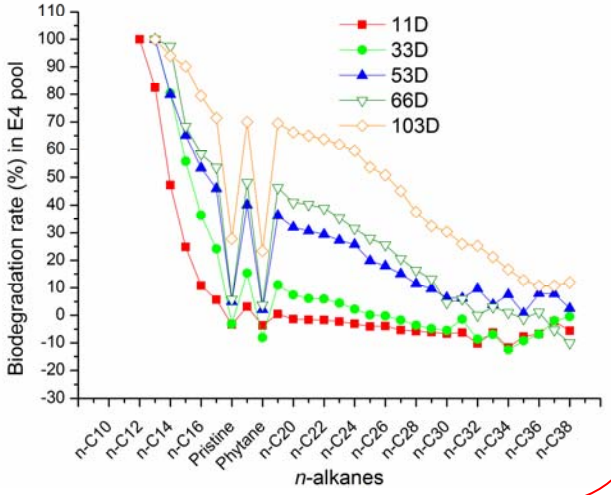

***n*-alkanes**

HDB(N1-4)

Biosurfactant

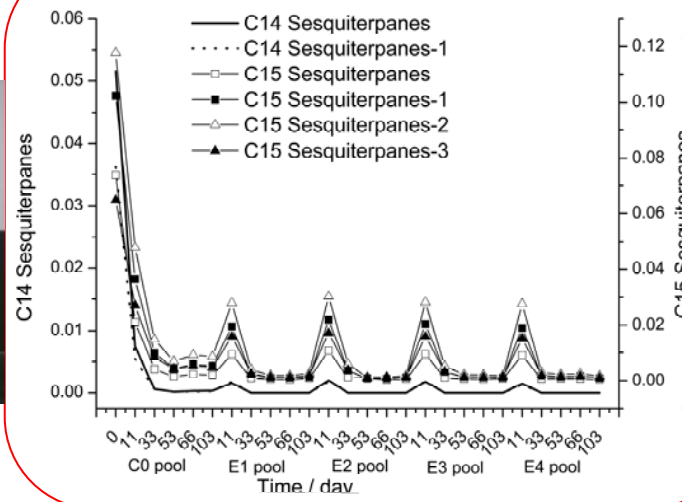

Biomarkers

Fermentation liquid

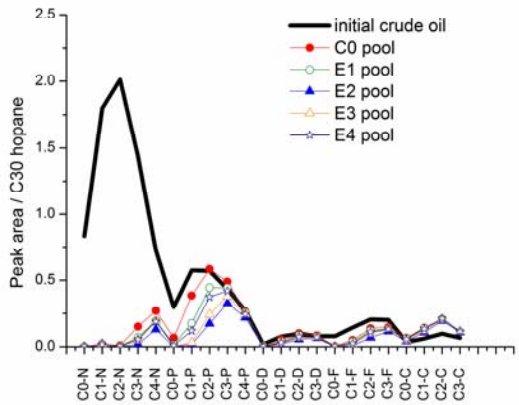

PAHs

Field simulated experiment

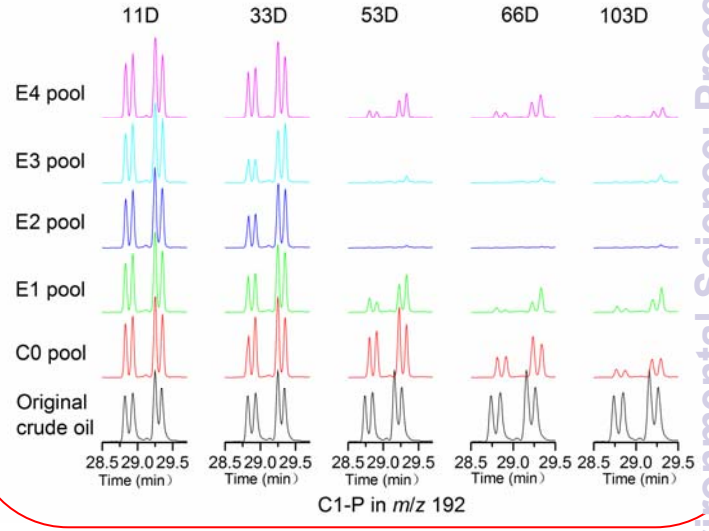

C1-P *m/z* 192

Environmental impact statement

This study presents the biodegradation effect of hydrocarbon degrading bacteria, rhamnolipid biosurfactants, and nutrients on the marine floating crude oil degradation for different hydrocarbons, including n-alkanes, polycyclic aromatic hydrocarbons (PAHs), and biomarkers.

Biodegradation of marine surface floating crude oil in a large-scale field simulated experiment

Mutai Bao [a,b*], Peiyan Sun [c,d*], Xiaofei Yang[c,d], Xinping Wang[c,d], Lina Wang[a,b], Lixin Cao [c,d], Fujuan Li [c,d]

[a] *Key Laboratory of Marine Chemistry Theory and Technology, Ministry of Education, Ocean University of China, Qingdao 266100, China*

[b] *College of Chemistry & Chemical Engineering, Ocean University of China, Qingdao 266100, China*

[c] *Key Laboratory of Marine Spill Oil Identification and Damage Assessment Technology, State Oceanic Administration, Qingdao 266033, China*

[d] *North China Sea Environmental Monitoring Center of State Oceanic Administration, Qingdao 266033, China*

Abstract

Biodegradations of marine surface floating crude oil with hydrocarbon degrading bacteria, rhamnolipid biosurfactants, and nutrients were carried out by a large-scale field simulated experiment in this paper. After 103-day experiment, for *n*-alkanes, the maximum biodegradation rate reached 71% and the results showed that it has comprehensive effect of hydrocarbon degrading bacteria, rhamnolipid biosurfactants, and nutrients. It also showed that rhamnolipid biosurfactants could shorten the biodegradation time through emulsifying function; the nutrients could greatly increase biodegradation rate by promoting HDB production. For PAHs, Chrysene series had higher weathering resistance. For the same series, the weathering resistance ability is C1- < C2- < C3- < C4-, After 53 days, no comprehensive effect occurred and more biodegradation was found for different *n*-alkanes in two pools which only added rhamnolipid

* **Corresponding author;** mtbao@ouc.edu.cn (M. Bao), Tel: +86-532-66782509, Fax: +86-532-6678254; sunpeiyan@bhfj.gov.cn (P. Sun), Tel: +86-532-58761006. M. Bao and P. Sun contributed equally to this paper. This is MCTL Contribution No. 25.

biosurfactants or nutrients, respectively. Except for C14, C15 and C16 sesquiterpanes, most of steranes and terpanes had high antibiodegradability.

***Keywords*:** large-scale field simulated experiment, floating crude oil, biodegradation rate, *n*-alkane, PAHs, biomarker

1. Introduction

Crude oil is an extremely complex compounds mainly consisting of aliphatics, aromatics and polar compounds. The number of oil spills is likely to increase resulted from the rapid development of ocean oil exploration and transportation. Once the oil spill released at sea, it is subject to various weathering processes, including microbial degradation.[1]

It is necessary to seek out a suitable technology to treat spilled oil. Bioremediation is an effective and economical method for further treatment of the oil spill contamination after adopting physical and chemical method.[2] Bioremeadiation relies on the hydrocarbon-degrading microbial consortium resident in the soil or water.[3,4] Generally, three enhanced bioremediation methods are used to clean up spilled oils: (1) adding biosurfactants, (2) treating oil with high efficient hydrocarbon degrading bacteria, or (3) applying nutrients such as nitrogen or phosphorous.[5,6]

In many cases, some isolated microorganisms can effectively degrade a single type of pollutants in lab conditions, however when introduced into real field conditions with multiple types of pollutants they often do not function as anticipated.[7] Therefore, mixed bacterial cultures were often designed and applied[4,8] to enhance biodegradation efficiency.

In this study, we report how to conduct biodegradation experiments of marine surface floating crude oil under large-scale field simulated conditions, and how to investigate the effect of

hydrocarbon degrading bacteria, rhamnolipid biosurfactants, and nutrients on the floating crude oil biodegradation for different hydrocarbons of *n*-alkanes, polycyclic aromatic hydrocarbons (PAHs), and biomarkers. A reliable GC-FID and GC-MS method was applied for identification and characterization of various groups of and individual petroleum hydrocarbons in biodegraded spill oil samples.[9] Furthermore, numerous diagnostic indices including *n*-alkanes, alkylated PAH homologues, and biomarkers were calculated and applied for unambiguous indication of the occurrence and estimation of degrees of oil biodegradation.

2. Materials and methods

2.1 Materials

The crude oil used in this experiment was obtained from Shengli Oilfield, China. The main physical properties of the crude oil are viscosity of 22.2 mPa.s (determined at 50^{o}C in 50 RPM), freezing point of 23 ^{o}C, and density of 0.8552 g cm^{-3}. Sixteen liters of crude oil was sprinkled evenly on the seawater surface of each pool.

The hydrocarbon degrading bacteria N1, N2, N3, and N4 used in this study were isolated from seawater samples collected from the coastal areas of Qingdao of China. The genera names were *Ochrobactrum* sp., *Brevibacillus parabrevis*, *B. parabrevis* and *B. parabrevis*, and the genbank accession numbers were HQ231209, HQ231210, HQ231211 and HQ231212, respectively.[10]

n-alkane calibration standards from *n*-C_9 to *n*-C_{36} and PAHs calibration standard mixtures were purchased from Sigma-Aldrich (St. Louis, MO, USA) and Restek (Bellefonte, PA, USA). *n*-alkane internal deuterated standard $C_{20}D_{24}$, terpanes and steranes internal standard 5-α-androstane and PAHs deuterated internal standards {[$^{2}H_{14}$]terphenyl (terphenyl-d_{14})} were purchased from Sigma-Aldrich (St. Louis, MO, USA). Biomarker terpane and sterane standards were obtained from Chiron (Trondheim, Norway). Ammonium sulfate, disodium hydrogen

phosphate and other chemicals used in laboratory were analytically pure, and used in the large-scale fermentation were all chemically pure.

Shimadzu GC-2010 with the FID detector and GC/MS-QP2010 (Kyoto, Japan) and a system control and data acquisition was achieved with a GC solution and GC/MS solution software, respectively. Experimetal fermenter (10 L) and large-scale factory fermenter (30 L, 1000 kg, and 10 000 kg), incubator, microscope (Leica DM1000), etc.

2.2 Fermentation

The fermentation culture medium for the hydrocarbon degrading bacteria N1-N4 and rhamnolipid biosurfactants contained 2.0 g paraffins, 3.0 g Na_2HPO_4, 3.0 g KH_2PO_4, 5.0 g $(NH_4)_2SO_4$, 0.5 g $MgSO_4$, 5.0 g NaCl, 0.02 g $CaCl_2$ and 1.0 g yeast powder per litter.

The fermentation procedures were as follows: 3 % (v/v) of the hydrocarbon degrading bacteria N1-N4 were inoculated in the enrichment medium and cultured for 3 days under the stirring rate of 120 rpm, 25°C, then inoculated into the fermentation culture medium and fermented for 3 days under the stirring rate of 120 rpm, 30 °C, about 6 000 kg Bacteria liquid was obtained. 3 % (v/v) of rhamnolipid biosurfactants production bacteria, which were stored in our lab, were innoculated on the concentrated culture medium and cultured for 3 days under the stirring rate of 120 rpm and temperature of 37°C, and then inoculated into the fermentation culture medium and fermented for 3 days at 30°C, about 4 000 kg rhamnolipid biosurfactants liquid was obtained.

The fermentation liquids were stored into 50 L plastic barrels using alcohol sterilized in advance. The barrels were labeled with the bacteria name and production time and stored in cool and airy storehouse, the air temperature was about 30ºC.

The fermentation liquids were inspected randomly on July 5th, 2009. The microbial population

in the plastic barrels was estimated by the most probable number (MPN) method using plate cultivation for the TVB and infectious microbe inspection. The percentage of the infectious microbe (mainly the yeasts and moulds) was below 1% and the concentration of TVB was more than 10^8 CFU·mL^{-1}. The fermentation liquids were both shallow milk yellow, transparent and had a normal smell. The floating substances with rich foam were obviously observed. Its emulsification effect of liquid paraffins was good.

2.3 Large-scale field simulated experiment

2.3.1. Experimental pool built and preparation. A large obsoleting hollow on the beach of Zhimai River estuary in Laizhou Bay, Shandong Province, China was chosen for this experiment. Six square pools with the same size were built in it. The side length of each pool was 400 cm (area of each pool: 16 m^2) and its depth was 120 cm, 30 cm clay mud was paved on the bottom of each pool horizontally and seawater was pumped to each pool at a depth of 70 cm. Six square pools are used for 1 blank pool (B0), 1 control pool (C0) and 4 experimental pools (E1, E2, E3, and E4), respectively.

The HDB fermentation broth was added (in 1.8 L m^{-2}) into experimental pools E1, E2, E3, and E4. Rhamnolipid biosurfactants were only added (in 1.2 L m^{-2}) into the experimental pools E2 and E4. $(NH_4)_2SO_4$ and KH_2PO_4 (mass ratio: 1:1) were applied as nutrients into E3 and E4 pools (in 0.6 g m^{-2}). The experimental designs were according to the results of laboratory mesocosm experiments.[10] The details of each pool were listed in Table 1.

2.3.2. Experimental Period, sampling frequency and weather condition. The duration for the experiments was 103 days, from July 12 to October 22, 2009. The first sampling was done on the July 12 and regarded as background, and then conduced the sampling on July 23 (11d), Aug. 14 (33d), Sep. 3 (53d), Sep. 16 (66d) and Oct. 22 (103d). During the experiment period, the

air temperature was high in July and August, and there were rainy in August, the daily highest air temperature reached over 30 ºC and the lowest over 20ºC. However, in September and October, the daily highest air temperature was reached to 19 ºC and the minimum to 9 ºC.

2.3.3. Monitoring index, sampling and analysis method. During the experiment, the monitoring indexes were conducted for the sea water and oil slick. The indexes for water were included the quantity of TVB and HDB. The fingerprinting for the oil slick was analyzed though GC-FID and GC-MS.

Oil film and water samples were collected in different pools for investigating changes of spilled oil and microorganisms. 250 mL sterilized wide-mouth glass jars and narrow-mouth bottles were used to collect oil film and water samples, respectively. Collected samples were placed into a container packed with ice bags and transported immediately to the laboratory for the instrumental analysis.

The samples for TVB and HDB analysis should be conducted under the aseptic condition. About 1000mL water sample under the surface 20 ~ 30 cm was collected in aseptic bottle, kept in cold storage and transported to the lab within 2 hours for analysis.

The number of microorganisms in the water samples was determined by the serial dilution technique in duplicate by the MPN method. [11, 12] In this experiment, we adopted three dilutions in triplicate. HDB were counted with standard mineral salt medium (MSM) agar plates using sterile crude oil as the sole source of carbon. The MSM contained 3 g NaCl, 3 g Na_2HPO_4, 2 g KH_2PO_4, 5 g $(NH_4)_2SO_4$, 0.7 g $MgSO_4 \cdot 7H_2O$ per liter. The pH was adjusted to 7.0-7.2 before sterilization. TVB were counted with standard agar plates using enrichment medium containing 3g of beef extract, 10g peptone, 5g NaCl and 3g agar per liter. The pH value was adjusted to 7.0-7.2 before sterilization.

The oil film samples were processed in the following procedure: 0.8 g oil from oil film samples was dissolved and diluted with hexane in a 10 mL volumetric flask. 200 μL of the solution was transferred into the sample bottle, added 500 μL hexane, 100 μL 100 μg mL^{-1} normal alkanes internal standard, 100 μL 10 μg mL^{-1} sterane and terpane internal standard, and 100 μL f 10 μg mL^{-1} PAHs internal standard, mixed them well for GC-MS and GC-FID analyses.

The *n*-alkanes were analyzed by GC-FID with a 30 m DB-5 capillary column (0.32 mm ID, 0.25μm film thickness). High purity nitrogen was used as carrier gas at a flow of 1.0 mL min^{-1}. Samples were injected in splitless mode. The oven temperature was programmed to start at 50 °C for 2 min, ramped to 300 °C at 6 °C per minute, and then held for 16 min. GC conditions were: injector temperature was 290 °C, and detector temperature was 300 °C.

The PAHs and biomarkers (sesquiterpanes, steranes and terpanes) were analyzed by GC-MS in full-scan mode to scan MS spectra for qualitative analysis and in the selected ion monitoring (SIM) mode for quantitative analysis. The column used was 30 m long (0.25 mm ID, 0.25 μm film thickness) DB-5MS capillary column. High purity helium was selected as the carrier gas, and its flow velocity was 1.0 mL min^{-1}. Samples were injected in splitless mode. The oven temperature was programmed to start at 50 °C for 2 min, ramped to 300 °C at 6 °C per minute, and then held for 16 min. GC-MS conditions were: injector temperature was 290 °C, interface temperature was 280 °C, ion source temperature was 230 °C.

2.4 Data analysis and degradation effect evaluation

n-alkanes, including pristane (Pr) and phytane (Ph), the weathering rate and biodegradation rate were used to evaluate weathering and biodegradation effect for control pool C0 and the experimental pool (E1, E2, E3 and E4), respectively.

The weathering rate (%) for the control pool C0 was calculated by formula (1).

The weathering rate (%) =($A_{\text{intial crude oil}}$ -A_{C0})/$A_{\text{intial crude oil}}$*100 (1)

A_{C0}: is hydrocarbon relative peak area (normalized to C30-17α (H), 21β (H)-hopane [13,14]) for control pool C0, $A_{\text{intial crude oil}}$： is hydrocarbon relative peak area (normalized to C30-17α (H), 21β (H)-hopane) for intial crude oil

The biodegradation rate (Percentage Lost, %) for the experimental pool (E1, E2, E3 and E4) was calculated by formula (2).

The biodegradation rate (%) =(A_{C0}-A_E)/A_{C0}*100 (2)

A_{C0}： is hydrocarbon relative peak area (normalized to C30-17α (H), 21β (H)-hopane) for control pool C0, A_E: is hydrocarbon relative peak area (normalized to C30-17α (H), 21β (H)-hopane) for experimental pool E1, E2, E3 and E4.

The degradation effect evaluation of PAHs was conducted by comparing relative peak area or peak height (relative to C30-17α (H), 21β (H)-hopane) of each component of the control pool C0 and experimental pools.

The biomarkers including terpanes and steranes, RSD of the relative peak area (relative to C30-17α (H), 21β (H)-hopane) of each component at different time for one pool was used to indicate whether it was degraded.

3. Results and discussion

3.1 Microbial growth

The total bacteria were counted with a standard agar plate. The hydrocarbon degrading bacteria were counted with a standard crude oil plate. The counting results of TVB and HDB are listed in Fig. 1.

It can be seen from Fig. 1 that there was a general trend in the profiles to go from a diminished number to an increased number, and then go back to a diminished number over time.

The number of HDB was decreased at the earlier stages, indicating that bacteria needed some time to adapt to the new environment. The number of HDB was increased after growing in the bioremediation test tank for about 11 d and all entered into stationary phase after 33 d. Compared with the control pool C0, the number of HDB in experimental pool E4 was multiplied 2 to 3 orders, the number of TVB in experimental pool E4 was multiplied 2 orders, which also demonstrated that the added HDB (N1-N4) grew and propagated in the experiment pools. The number of HDB and TVB in E4 pool were kept 10^5 and 10^6 CFU·mL^{-1} on 103 d, respectively.

3.2 *n*-alkanes and the characteristic ratios

3.2.1. *n*-alkanes, including pristane and phytane. The weathering effect and biodegradation assessment of *n*-alkanes, including Pristane (Pr) and Phytane (Ph) under field natural conditions at different time was shown in Fig. 2.

Fig. 2a showed the weathering effect of *n*-alkanes in control pool C0 in natural weathering process (including evaporation, emulsification, dissolution, photo-Oxidation and natural biodegratdation etc). The air temperature was very high from July 11 to August 14 (33d), the highest temperature was more than 30 ^{o}C and the lowest temperature was more than 22 ^{o}C. During this period, the evaporation was the principal weathering process. So, all *n*-alkanes from *n*-C9 to *n*-C12 almost disappeared after 11d. 33 d later, the *n*-alkanes from *n*-C17 to *n*-C30 were most affected heavily by weathering process with the weathering rate of 30 ~ 40 %. With the similar weathering rate trend for *n*-C17 and Pr, *n*-C18 and Ph, it also showed that the evaporation was the one of the main influence factors. [15] From 11d to 66d, the *n*-alkanes from *n*-C17 to *n*-C38 presented a similar variance for their weathering rate. While at 103 d, an increasing trend was shown for the *n*-alkanes up to *n*-C31 weathering rate, especially for *n*-C36, *n*-C37, *n*-C38 (the weathering rate is above 50%), yet the lowest weathering rate occurred was even negative for

n-alkanes from *n*-C17 to *n*-C30 .

Figs.2b, 2c, 2d, and 2e showed the biodegradation effects on *n*-alkanes in experimental pool E1, E2, E3 and E4. The biodegradation rate of *n*-alkanes up *n*-C19 showed a decreasing trend as a whole in these four experimental pools. For the different experimental pools, the maximum biodegradation rate of *n*-alkanes was present at different time in E1 (103 d), E2 (53 d), E3 (66 d), and E4 (103 d) pool, respectively. The rhamnolipid biosurfactants could emulsify the crude oil into the oil film, increasing the contact area between microorganism and the crude oil, hence the biodegradation time was shorten.[16] So the maximum biodegradation was present earlier in experimental pool E2 than that in others. For the E3 and E4 pools which were added with the nutrients, since the nutrients could promote HDB production and largely increased biodegradation rate in a certain time, the biodegradation rate of *n*-alkanes in E3 and E4 after 33d was positive and greater than that after 11d, although the biodegradation rate of *n*-alkanes in C0 after 33d was very satisfied which was different from that in E1 and E2 (most of loss rate was negative).

E4 pool (Fig. 2e) was added rhamnolipid biosurfactants and nutrients. The biodegradation rate of the *n*-alkanes showed their comprehensive effect compared with that of E1, E2 and E3. During the 103-day experimental period, the biodegradation rate of almost all the *n*-alkanes was increasing with time. The biodegradation rate of the lighter *n*-alkanes less than *n*-C17 was enhanced obviously after 33d relative to that of the *n*-alkanes up to *n*-C17. The biodegradation degree of *n*-alkanes longer than *n*-C15 was obviously stimulated from 53 d to 66 d, significantly higher than that of 33 d ago, about 18% increased. Its biodegradation rate has reached 54 % at 66d, which was greater than E2 (maximum 48% at 53d), similar to E1 (maximum 54% at 103d) and a little less than E3 (maximum 56% at 66d). What's more, after 103d, its biodegradation rate reached 71%. This demonstrated that the overall effect of nutrients, rhamnolipid biosurfactants

and HDB were favoring biodegradation oil spills.[16]

3.2.2. The characteristic ratios. The effect of microbial degradation could be monitored by the ratios of Pristane / *n*-C_{17} (Pr / *n*-C17), Phytane / *n*-C_{18} (Ph / *n*-C18), and (Pristane + Phytane) / (*n*-C17 + *n*-C18) [(Pr + Ph) / (*n*-C_{17} + *n*-C_{18})] (Fig. 3). Of course, these ratios may underestimate the extent of biodegradation due to the fact that Pr and Ph could also be degraded under severe weathering conditions during a long period.[17, 18] The characteristic ratios in the control pool C0 were quite stable and almost did not change with time, which implied that *n*-C_{17} and Pr, *n*-C_{18} and Ph had similar weathering effect, especially evaporation due to their similar molecular weight. In experimental pools of E1, E2, E3, and E4, the characteristic ratios were increased evidently, which clearly showed the difference biodegradation effect on *n*-C_{17} and Pr, *n*-C_{18} and Ph. *n*-C_{17} and *n*-C_{18} were more easily biodegraded than Pr and Ph. The change trend of the characteristic ratios in experimental pools of E1, E2, E3, and E4 was similar to the biodegradation rates of *n*-alkanes.

Fig.3 showed that Pr / *n*-C17 in E1, E2, E3, and E4 increased by 72%, 49%, 33%, and 149%, Ph / *n*-C_{18} increased by 74%, 46%, 53%, and 158%, (Pr + Ph) / (*n*-C_{17} + *n*-C_{18}) increased by 69%, 44%, 48%, and 148%, respectively, which the values were all relative to that of the initial crude oil. But the newly research results showed that Pr / *n*-C_{17}, Ph / *n*-C_{18} could be decreased under sulphate reducing conditions, in which the degradation of Pr and Ph played a key role under this condition.[19]

The ratios of Pr / Ph in experimental pools E1, E2, E3, and E4 showed strong weathering resistance and stability, which was similar to those in the control pool C0 during the 103 d experimental periods. But owing to the effects of both weathering and biodegradation, Pr / Ph couldn't be used reliably as a conservative source marker for moderately biodegraded samples.[20]

These results indicated that *n*-C_{17} and *n*-C_{18} were obviously biodegraded. The long-chain *n*-alkanes of C_{17} and C_{18} could also be the preferred substrates for fast biodegradation, and *n*-C_{17} was the most preferred substrate, [21] which mainly due to the effect of the enzymatic degradation reactions and temperature.

3.3 PAHs

The PAHs in the crude oil were mostly the C_1 to C_4 alkylated homologues of their parent PAHs components, among which the most dominant are naphthalene (N), phenanthrene (P), dibenzothiophene (D), fluorine (F), and chrysene (C). [22]

Fig. 4 showed the relative peak area（relative to C30-17α (H), 21β (H)-hopane）of the five target petroleum characteristic alkylated PAH homologues included naphthalenes (C0-N, C1-N, C2-N, C3-N, and C4-N), phenanthrenes (C0-P, C1-P, C2-P, C3-P, and C4-P), dibenzothiophenes (C0-D, C1-D, C2-D, C3-D), fluorenes (C0-F, C1-F, C2-F, and C3-F), and chrysenes (C0-C, C1-C, C2-C, and C3-C) in the control pool C0 and experimental pools at different time.

Fig. 4a showed the variation of C1 to C4 alkylated homologues of naphthalene, phenanthrene, dibenzothiophene, fluorine, and chrysene in 53d. Compared with original crude oil, the relative peak area of other four PAHs series presented decreasing trend, apart from chrysene series with an obvious increasing trend. That proved chrysene series with higher weathering resistance. [8] For the same series, the ability of weathering resistance is C1 - < C2 - < C3 - < C4 - . Compared with experimental E1, E2, E3 and E4, the effect by biodegradation was E2 > E3 > E4 > E1 at 53d, 66d and 103d, which was also presented in Fig.4c and Fig.4d. This phenomenon was different with *n*-alkanes and showed the complexity of degradation for PAHs. This should be given much more attention.

The naphthalene series were most vulnerable to the impact of weathering process (Fig. 4b). It

showed that naphthalene disappeared completely mainly due to evaporation. C1- Naphthalene decreased from 1.8 to 0.05 in C0 pool, to 0.02 in the experimental pools, and all decreased to 0.01 at 33 d. The relative peak area of C2 - N, C3 - N and C4 - N was reduced significantly in 11 days, C2-N from 2.01 to less than 0.34 in C0 pool, to less than 0.16 (E1:0.13, E2: 0.16, E3:0.13, E4:0.14) in the experimental pools; C3-N from 1.44 to less than 0.66 in C0 pool, to less 0.51 (E1: 0.47, E2: 0.51, E3:0.47, E4:0.49) in the experimental pools; C4-N from 0.72 to less than 0.51 in C0 pool, to less 0.45(E1: 0. 43, E2: 0.45, E3:0.43, E4:0.44) in the experimental pools. After 33 d, the relative peak area of C2 - N, C3 - N, C4 - N all decreased to less than 0.04, 0.28, 0.35 in the control pool C0 and less than 0.01, 0.17 and 0.28 in experimental pools. The relative peak area of N series in E4 showed decreasing trend, compared with that in E1, E2 and E3.The decreasing degradation order from C0-N to C4-N was also proven in the results in Figure 5a.

Fig.4c and Fig.4d respectively showed C1-P variation at *m*/*z* 192 mass chromatograph including 3-,2-,9-/4-,1-methylphenanthrene and C1-D variation at *m*/*z* 198 mass chromatograph including 4-,3-,1-methyldibenzothiophene. The weathering degradation of 3-,2-,9-/4-methylphenanthrene and 4-,3-,1-methyldibenzothiophene were biodegraded distinctly after 33 days. 2, 3-methylphenanthrene disappeared in E2 and E3 pools after 53 d, 9-/4-methylphenanthrene was also biodegraded markedly. The order of biodegradation effect in experimental pools was E2 > E3 > E4 > E1 after 53days.

3.4 Biomarkers

The steranes with small molecular weight were more easily subjected to weathering. Fig. 5 confirmed that C14, C15, and C16 sesquiterpanes were vulnerable to weathering. After 11 d, the relative content of C14, C15, and C16 sesquiterpanes were greatly decreased, which demonstrated that the evaporation effect was mainly applied to the hydrocarbons of low molecular weight. After

33d, C14 sesquiterpanes, C14 sesquiterpanes-1, C15 sesquiterpanes, C16 sesquiterpanes, and C16 sesquiterpanes-2 all disappeared in all pools. Compared with the control pool C0, the relative content of C15 sesquiterpanes-1, C15 sesquiterpanes-2, C15 sesquiterpanes-3, C16 sesquiterpanes-1, C16 sesquiterpanes-3 in experimental pools were lower due to the biodegradation effect, the maximum degradation rates were 88%, 85%, 81%, 71%, and 65%, respectively.

Table 2 summarized the statistic of relative peak area for tricycle diterpanes, hopanes, and steranes (normalized to C30-17α (H), 21β (H)-hopane) in the control pool C0 and the experimental pools of E1, E2, E3, and E4. From Table 2, there were only 5 biomarkers, C21-13b(H),14a(H)- tricycle diterpanes, C22-13b(H), 14a(H) - tricycle diterpanes, gammacerane, 22R - 17a(H), 21b(H) - pentakishomohopane and 20S - 5a(H), 14b(H), 17b(H) - cholestane, which RSD (relative standard deviations) exceeded 10%, with the biggest value of 13.13%. About 47% components' RSD were under 5%, 79% components' RSD were under 7%. These confirmed that these steranes were resistance to biodegradability.

4. Discuission

Oil spills can have long-lasting and devastating effects on the ocean environment, especially the 2010 Deepwater Horizon Oil Spill.[23] Therefore, seeking for effective measures of cleaning up oil spills on the ocean has become an urgent issue. When oil spill occurs, the first step is the physical removal, and then using chemical treating agents to disperse or emulsify the oil.[24]

Bioremediation is an effective and economical method for the recovery of the residual oil spill and marine environment. Understanding the different effect and contribution of hydrocarbon degrading bacteria, biosurfactants, and nutrients to the oil spill biodegradation has been

considered an important component in developing oil spill bioremediation countermeasures.

This study provides large-scale field simulated biodegradation experiments of marine surface floating crude oil on the basis of the laboratory experiments,[10, 13] and discusses the different effect of hydrocarbon degrading bacteria, rhamnolipid biosurfactants, and nutrients on the floating crude oil biodegradation for different hydrocarbons of *n*-alkanes, PAHs, and biomarkers.

Acknowledgements

This research were supported by "The National Natural Science Foundation of China" (41376084); "Program for New Century Excellent Talents in University" (NCET-11-0464); "The Development Program of Science and Technology in Shandong Province" (2011GHY11522); "The Open Foundation of Key Laboratory of Marine Spill Oil Identification and Damage Assessment Technology of SOA" (201402). This is MCTL Contribution No. 25.

References

1. M. Kim, S. H. Hong, J. Wona, U. H. Yim, J. H. Jung, S. Y. Ha, J. G. An, C. Joo, E. Kim, G. M. Han, S. Baek, H-W. Choi, W. J. Shim, Petroleum hydrocarbon contaminations in the intertidal seawater after the Hebei Spirit oil spill -- Effect of tidal cycle on the TPH concentrations and the chromatographic characterization of seawater extracts, *Water Res.*, 2013, 47, 758-768.
2. R. M. Atlas, Petroleum biodegradation and oil spill bioremediation, *Mar. Pollut. Bull.*, 1995, 31, 178-182.
3. S. Supaphol, S. Panichsakpatana, S. Trakulnaleamsai, N. Tungkananuruk, P. Roughjanajirapa, A. G. Ödonnell, The selection of mixed microbial inocula in environmental biotechnology: example using petroleum contaminated tropical soils, J. Microbiol Meth., 2006, 65, 432-44.

4. H. S. Joo, P. M. Ndegwa, M. Shoda, C. C. Phae, Bioremediation of oil-contaminated soil using Candida catenulate and food waste, *Environ. Pollut.*, 2008, 156, 891-896.

5. A. J. Mearns, Cleaning Oiled Shores: Putting bioremediation to the test, *Spill Sci. Technol. Bull.*, 1997, 4, 209-217.

6. R. C. Prince, R. R. Lessard, J. R. Clark, Bioremediation of marine oil spills, *Oil Gas Sci. Technol.*, 2003, 58, 463-468.

7. A. C. Singer, C. J. van der Gast, I. P. Thompson, Perspectives and vision for strain selection in bioaugmentation, *Trends Biotechnol.*, 2005, 23, 74-77.

8. Z. D. Wang, M. Fingas, S. Blenkinsopp, G. Sergy, M. Landriault, L. Sigouin, J. Foght, K. Semple, D. W. S. Westlake, Comparison of oil composition changes due to biodegradation and physical weathering in different oils, *J. Chromatogr. A*, 1998, 809, 89-107.

9. P. Y. Sun, M. T. Bao, Z. H. Gao, G. M. Li, X. P. Wang, Y. H. Zhao, Q. Zhou, L. X. Cao, Fingerprinting and source identification of an oil spill in China Bohai Sea by gas chromatography-flame ionization detection and gas chromatography–mass spectrometry coupled with multi-statistical analyses, *J. Chromatogr. A*, 2009, 1216, 830-836.

10. M. T. Bao, L. N. Wang, P. Y. Sun, L. X. Cao, J. Zou, Y. M. Li, Biodegradation of crude oil using an efficient microbial consortium in a simulated marine environment, *Mar. Pollut. Bull.*, 2012, 64, 1177-1185.

11. K. Bartscht, H. Cypionka, J. Overmann, Evaluation of cell activity and of methods for the cultivation of bacteria from a natural lake community, *FEMS Microbiol. Ecol.*, 2006, 28, 249-259.

12. M. Nikolopoulou, N. Pasadakis, N. Kalogerakis, Enhanced bioremediation of crude oil utilizing lipophilic fertilizers, *Desalination*, 2007, 211: 286-295.

13. K. E. Peters, and J. M. Moldowan, The biomarker Guide: interpreting molecular fossils in petroleum and ancient sediments, Prentice Hall, Englewood Cliffs, 1993. 363.

14. W. K. Seifert, J. M. Moldowan, The effect of biodegradation on steranes and terpanes in crude oils, *Geochim. Cosmochim.*, 1979, 43, 111-126.

15. Z. D. Wang, M. Fingas, Development of oil hydrocarbon fingerprinting and identification techniques, *Mar. Pollut. Bull.*, 2003. 47, 423-452.

16. Q. G. Chen, M. T. Bao, X. N. Fan, S. K. Liang, P. Y. Sun, Rhamnolipids enhance marine oil spill bioremediation in laboratory system, *Mar. Pollut. Bull.*, 2013, 71, 269-275.

17. J. F. Rontani, P. Bonin, Production of pristane and phytane in the marine environment: role of prokaryotes, *Res. Microbiol.*, 2011, 162, 923-933.

18. F. D. Bost, R. Frontera-Suau, T. J. McDonald, K. E. Peters, P. J. Morris, Aerobic biodegradation of hopanes and norhopanes in Venezuelan crude oils, *Org. Geochem.*, 2001, 32**,** 105-114.

19. M. Hasingera, K. E. Scherra, T. Lundaaa, L. Bräuerc, C. Zachc, A. P. Loibnera, Changes in iso- and n-alkane distribution during biodegradation of crude oil under nitrate and sulphate reducing conditions, *J. Biotechnol.*, 2012, 157, 490-498.

20. C. P. McIntyre, P. McA. Harvey, S. Ferguson, A.M. Wressnig, I. Snape, S.C. George, Determining the extent of weathering of spilled fuel in contaminated soil using the diastereomers of pristane and phytane, *Org. Geochem.*, 2007, 38, 2131-2134.

21. M. Binazadeh, I. A. Karimi, Z. Li, Fast biodegradation of long chain n-alkanes and crude oil at high concentrations with Rhodococcus sp. Moj-3449, *Enzyme Microb. Tech.*, 2009, 45, 195-202.

22. Z. Z. Zhou, Z. F. Liu, L. D. Guo, Chemical evolution of Macondo crude oil during

laboratory degradation as characterized by fluorescence EEMs and hydrocarbon composition, *Mar. Pollut. Bull.*, 2013, 66, 164-175.

23. Y. Y. Gonga, X. Zhao, Z. Q. Cai, S. E. O'Reilly, X. D. Hao, D. Y. Zhao, A review of oil, dispersed oil and sediment interactions in the aquatic environment: Influence on the fate, transport and remediation of oil spills, *Mar. Pollut. Bull.*, 2014. 79, 16-33.

24. H. Toyoharu, T. Hiroaki, K. Masakazu, Bioremediation on the Shore after an Oil Spill from the Nakhodka in the Sea of Japan. I. Chemistry and Characteristics of Heavy Oil Loaded on the Nakhodka and Biodegradation Tests by a Bioremediation Agent with Microbiological Cultures in the Laboratory, *Mar. Pollut. Bull.*, 2000. 40, 308-314.

Fig. 1. The total viable bacteria (TVB) and hydrocarbon-degrading bacteria (HDB)

Fig. 2. The *n*-alkanes degradation rate in control pool (C0) and the experimental pools (E1, E2, E3, and E4)

(a) Weathering effect of *n*-alkanes in control pool C0, (b) Biodegradation effect of *n*-alkanes in experimental pool E1, (c) Biodegradation effect of *n*-alkanes in experimental pool E2, (d) Biodegradation effect of *n*-alkanes in experimental pool E3, (e) Biodegradation effect of *n*-alkanes in experimental pool E4.

Fig. 3. The characteristic ratios of Pr / n-C17, Ph / n-C18, and (Pr + Ph) / (n-C17+ n-C18) of intial crude oil, weathering pool B1, and experimental pools E1, E2, E3, and E4

Fig. 4. The target alkylated PAHs homologues (naphthalene series, phenanthrene series, dibenzothiophene series, fluorine series and chrysene series) in intial crude oil, control pool C0, and experimental pools E1, E2, E3, and E4

(a) The variation of C1 to C4 alkylated homologues of naphthalene, phenanthrene, dibenzothiophene, fluorine, and chrysene in 53d, (b) The variation of naphthalene series, (c) The variation of C1-P in *m*/*z* 192 mass chromatograph, (d) The variation of C1-D in *m*/*z* 198 mass chromatograph.

Fig. 5. C14, C15, C16 sesquiterpane series of intial crude oil, control pool C0, and experimental pools E1, E2, E3, and E4

(a) The variation of C14, C15 sesquiterpane series, (b) The variation of C16 sesquiterpane series

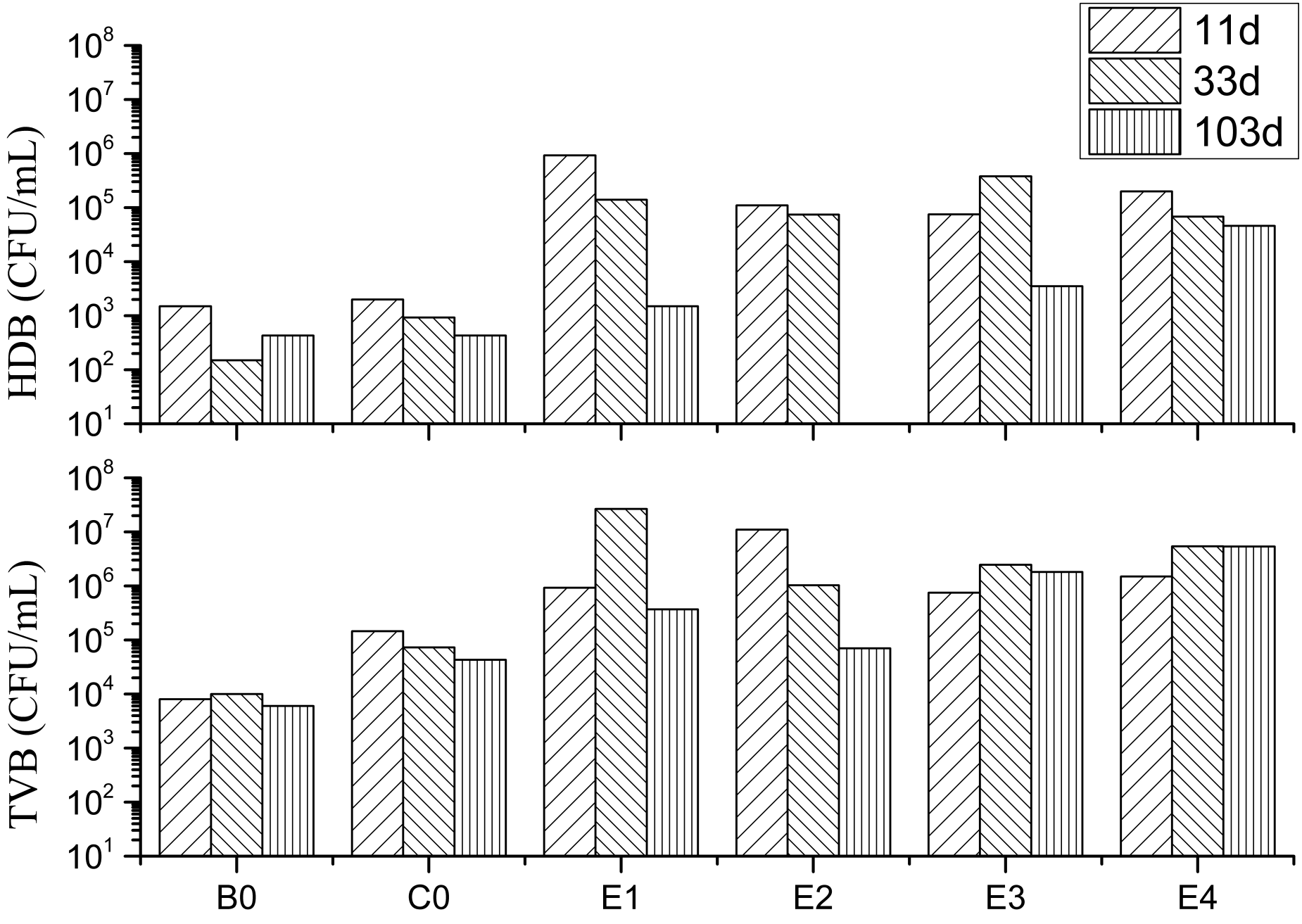

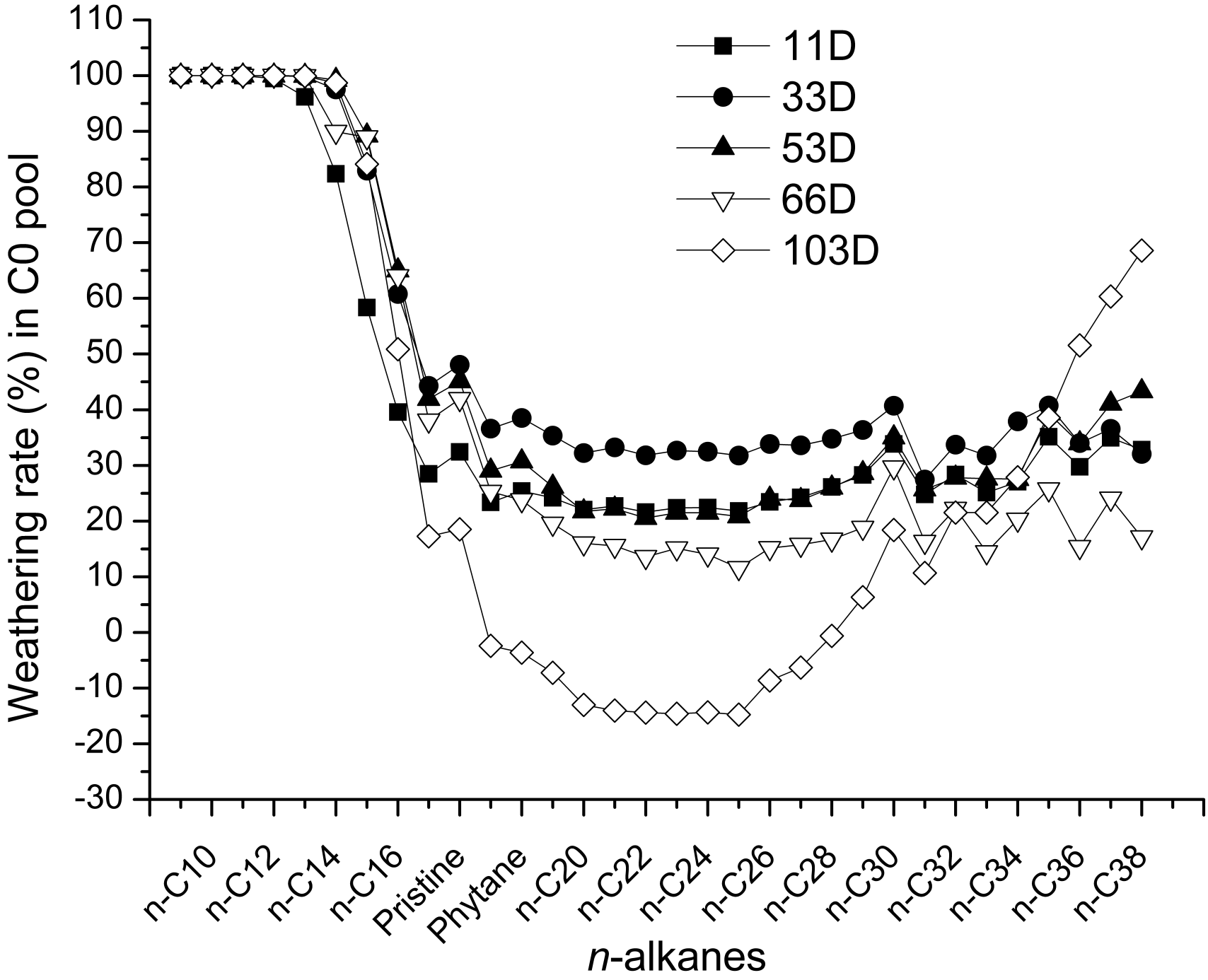

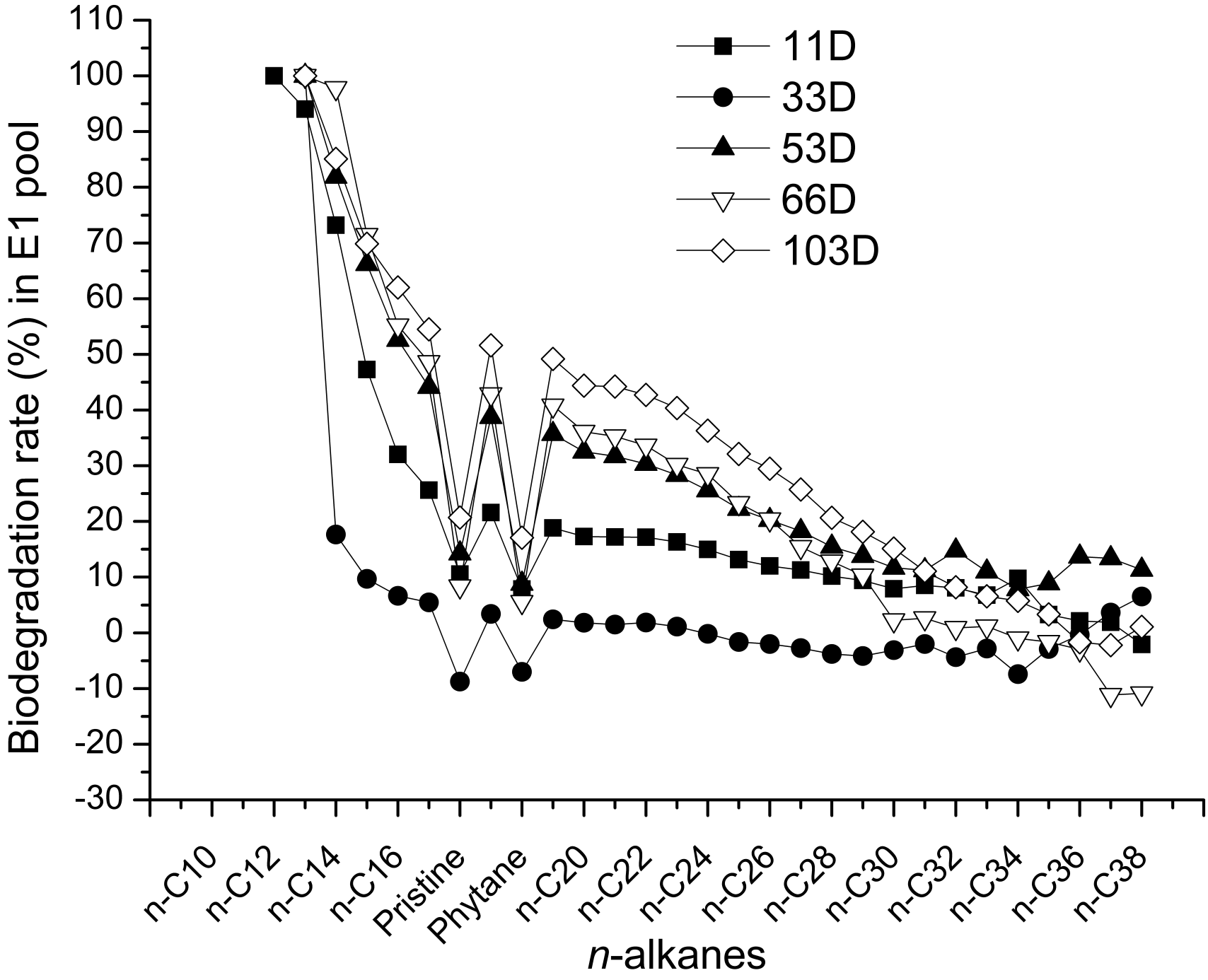

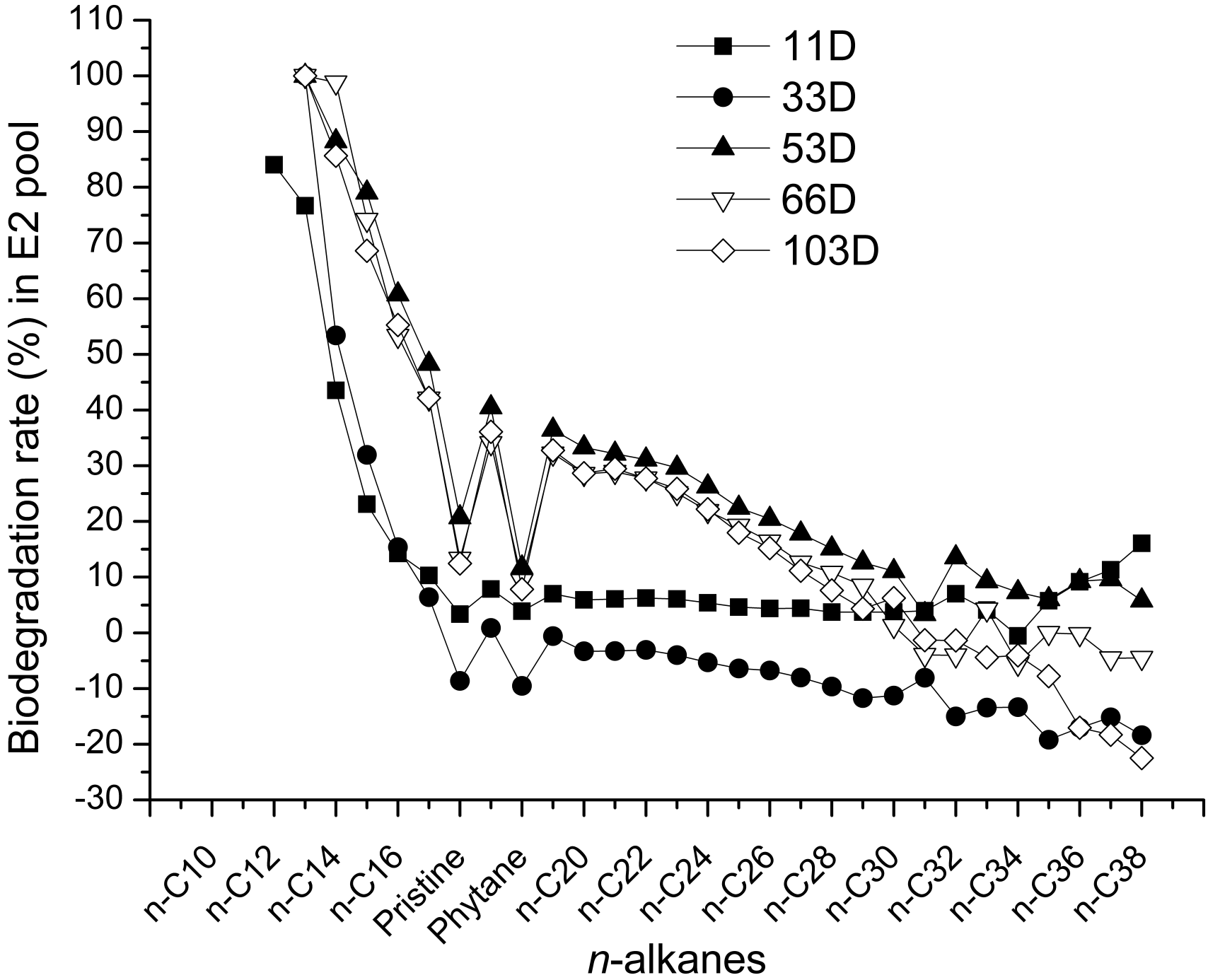

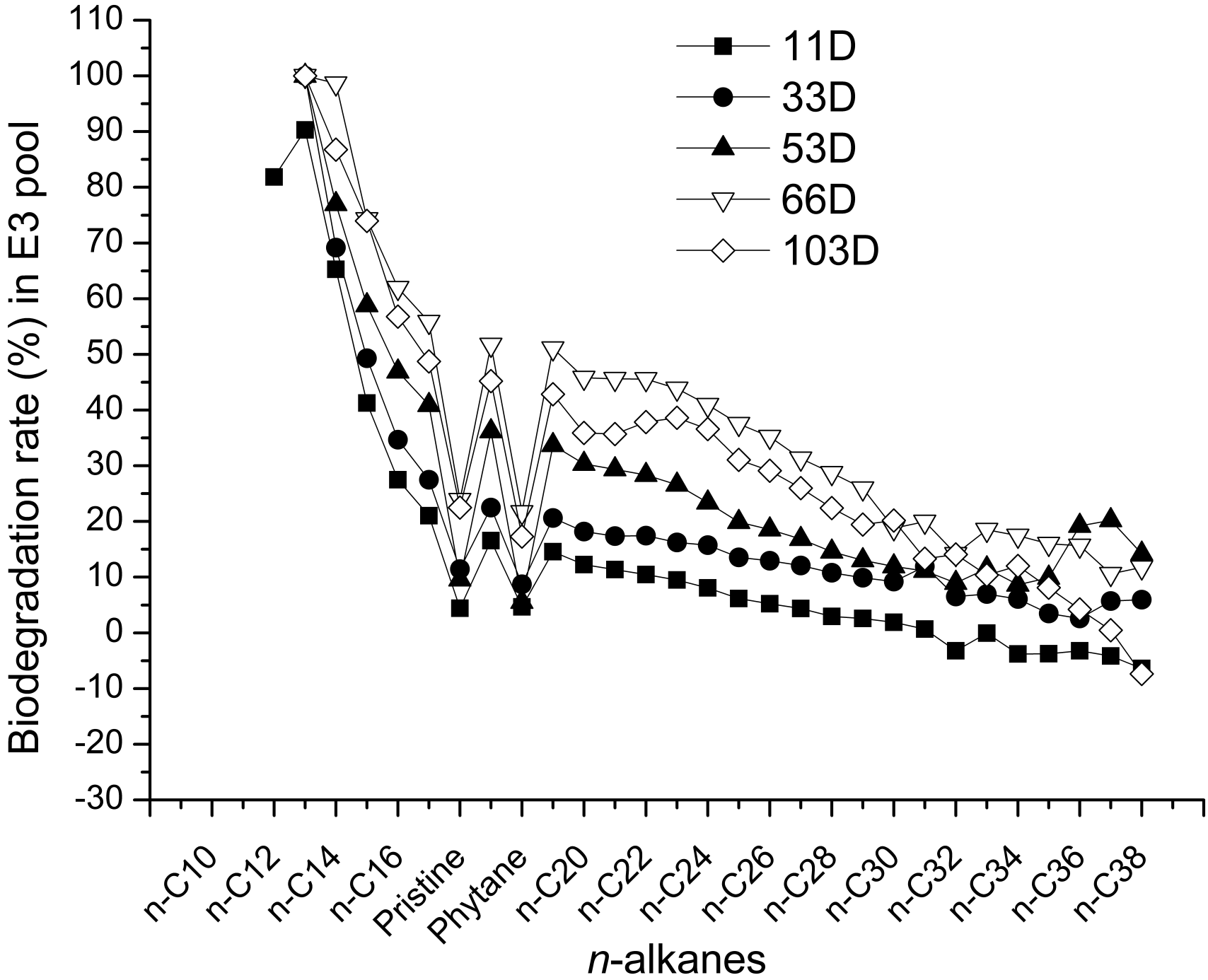

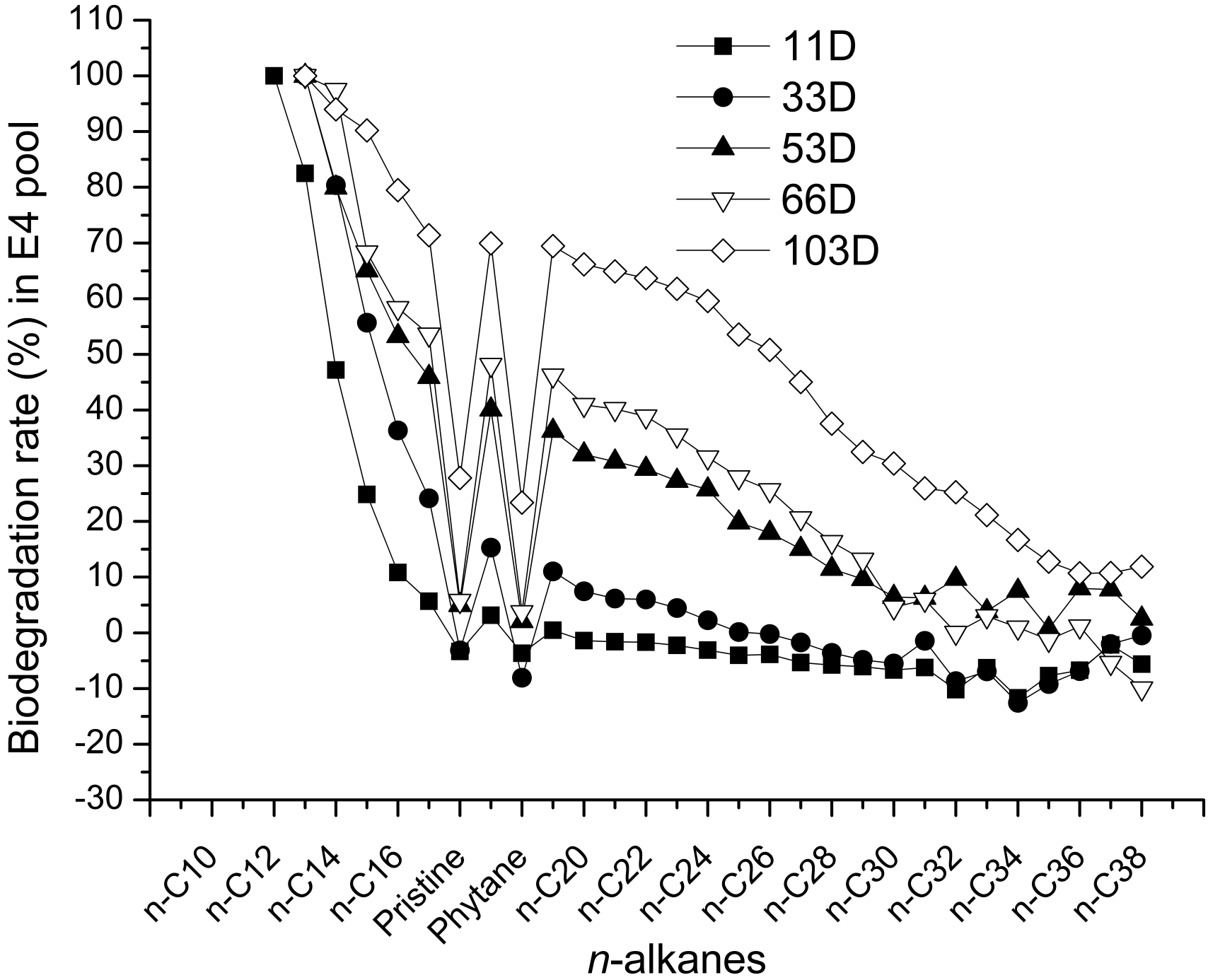

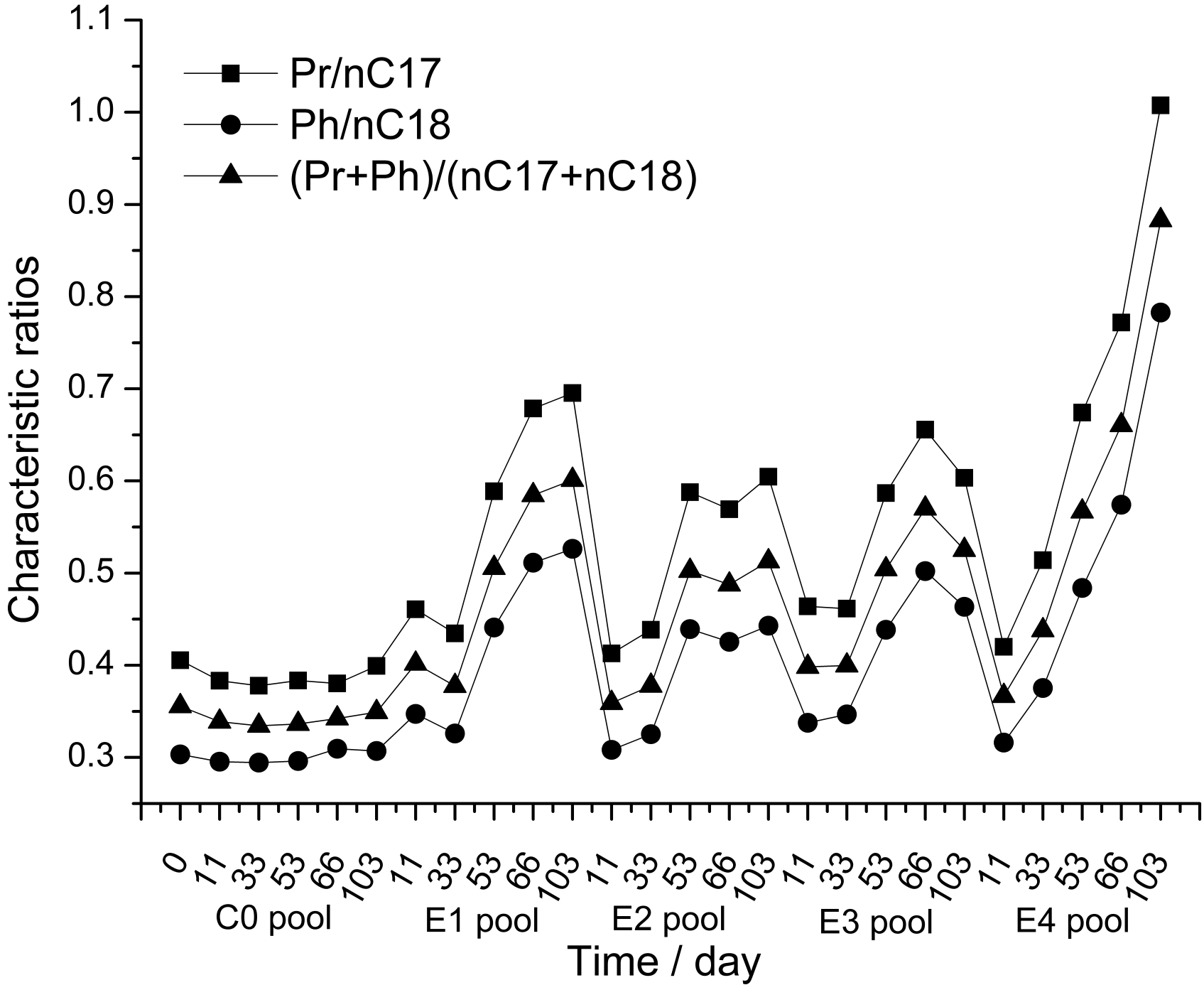

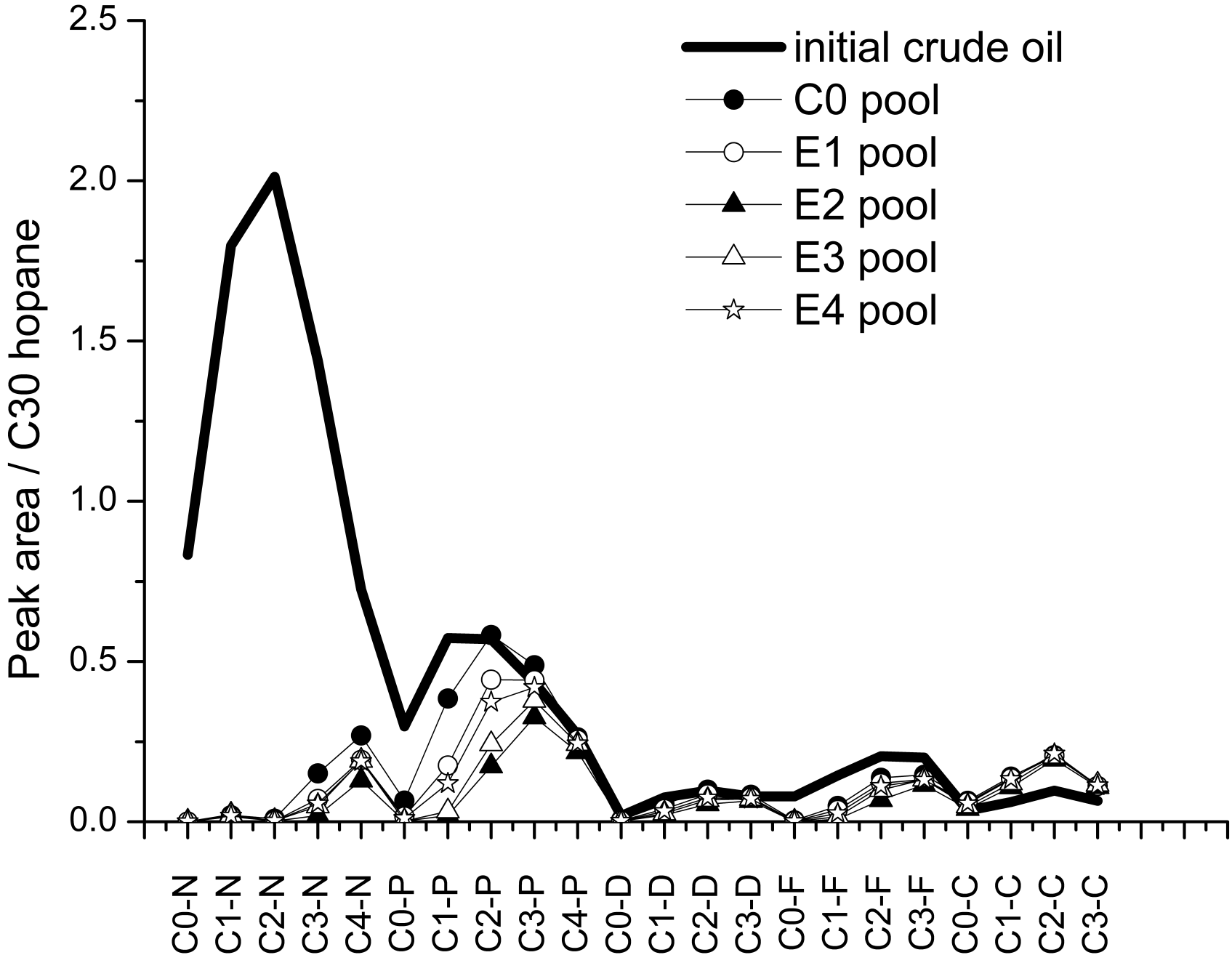

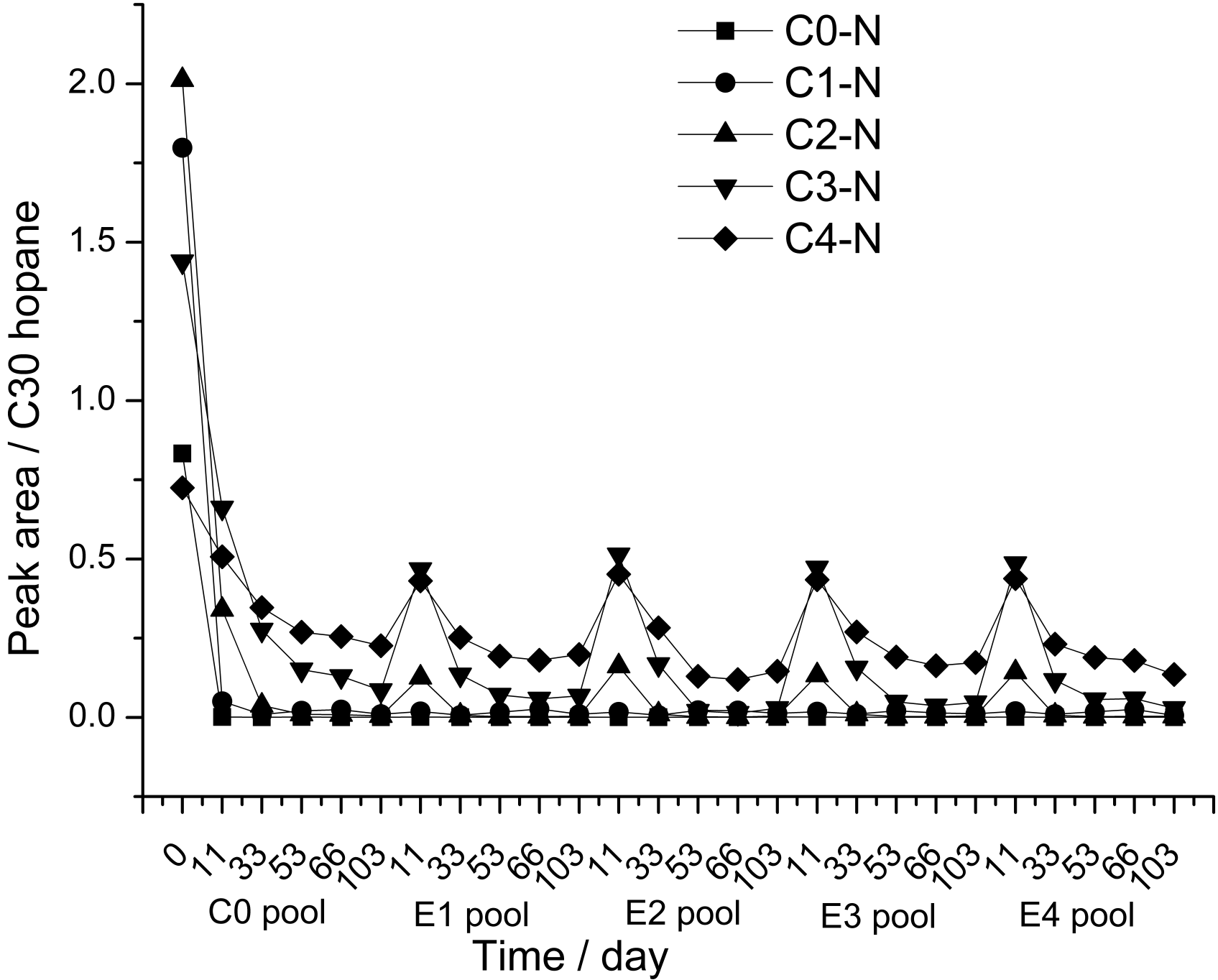

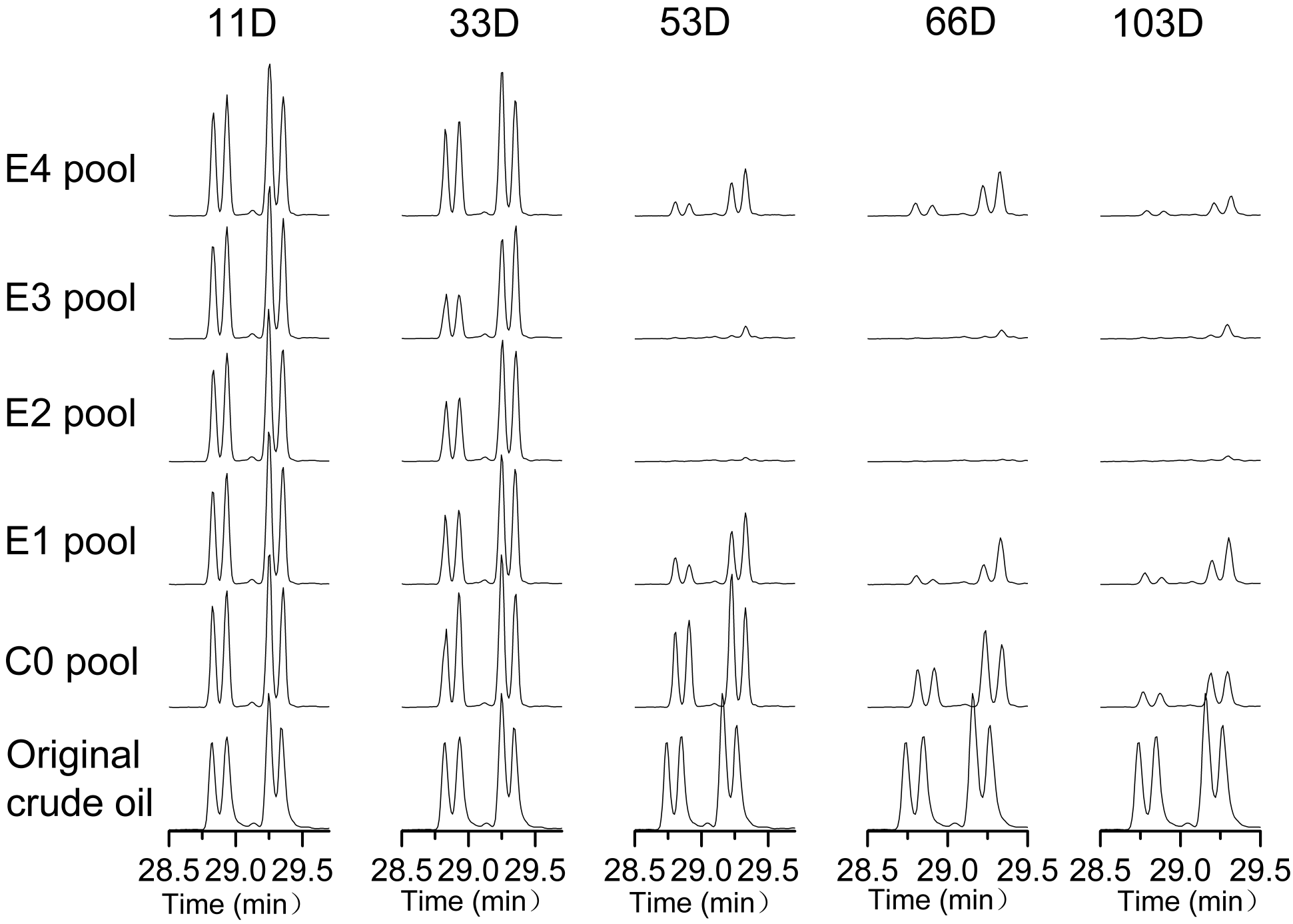

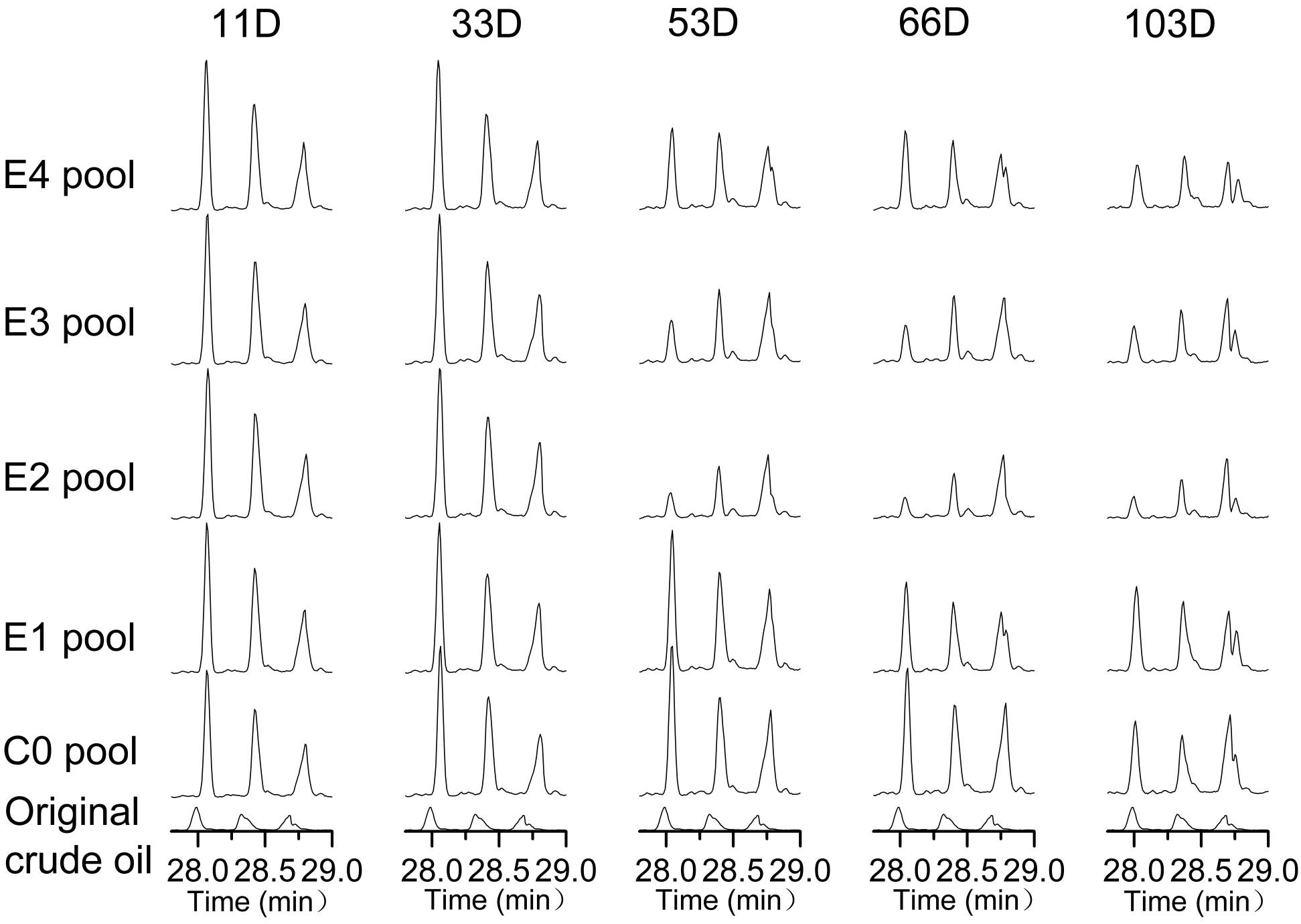

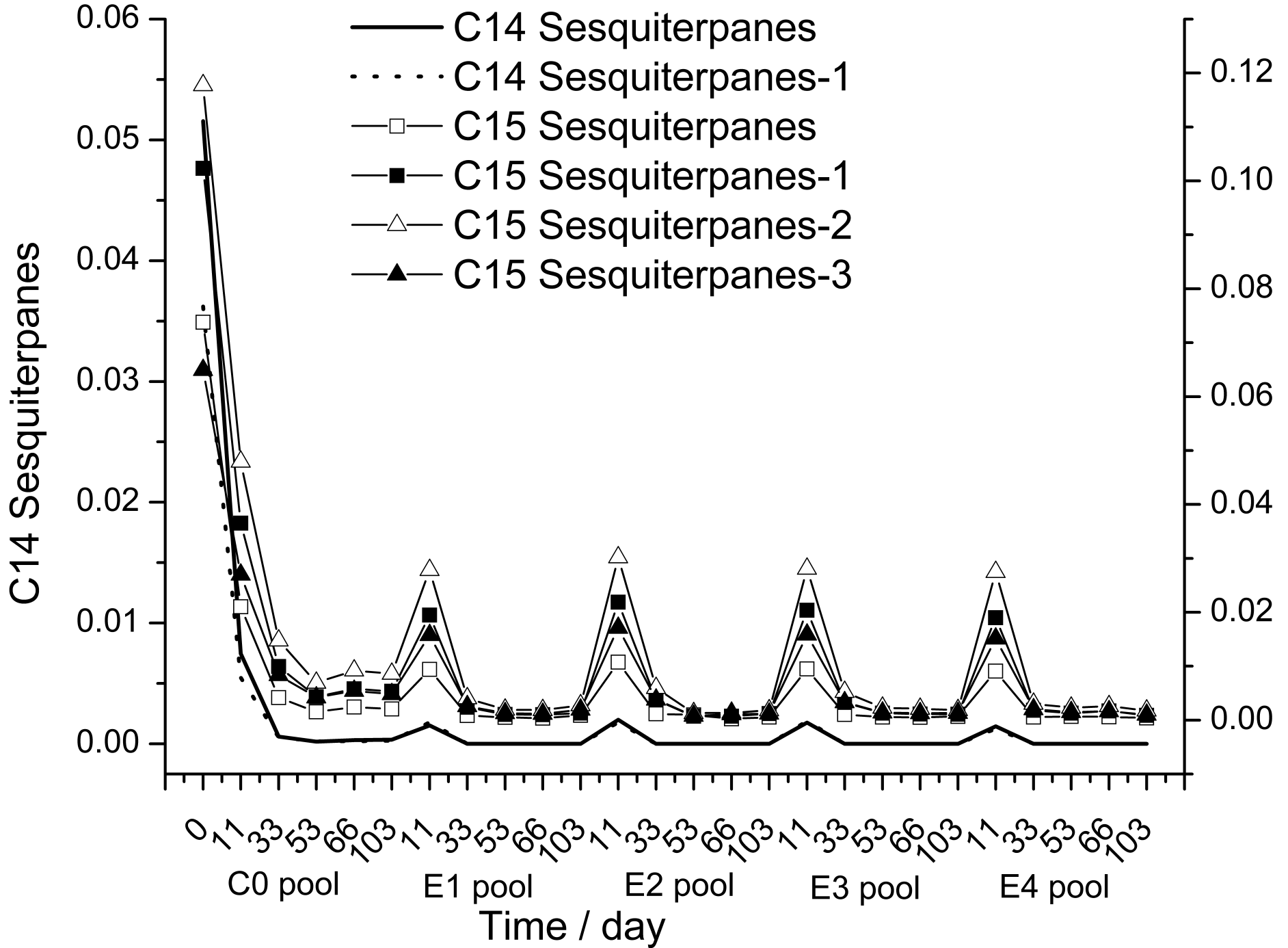

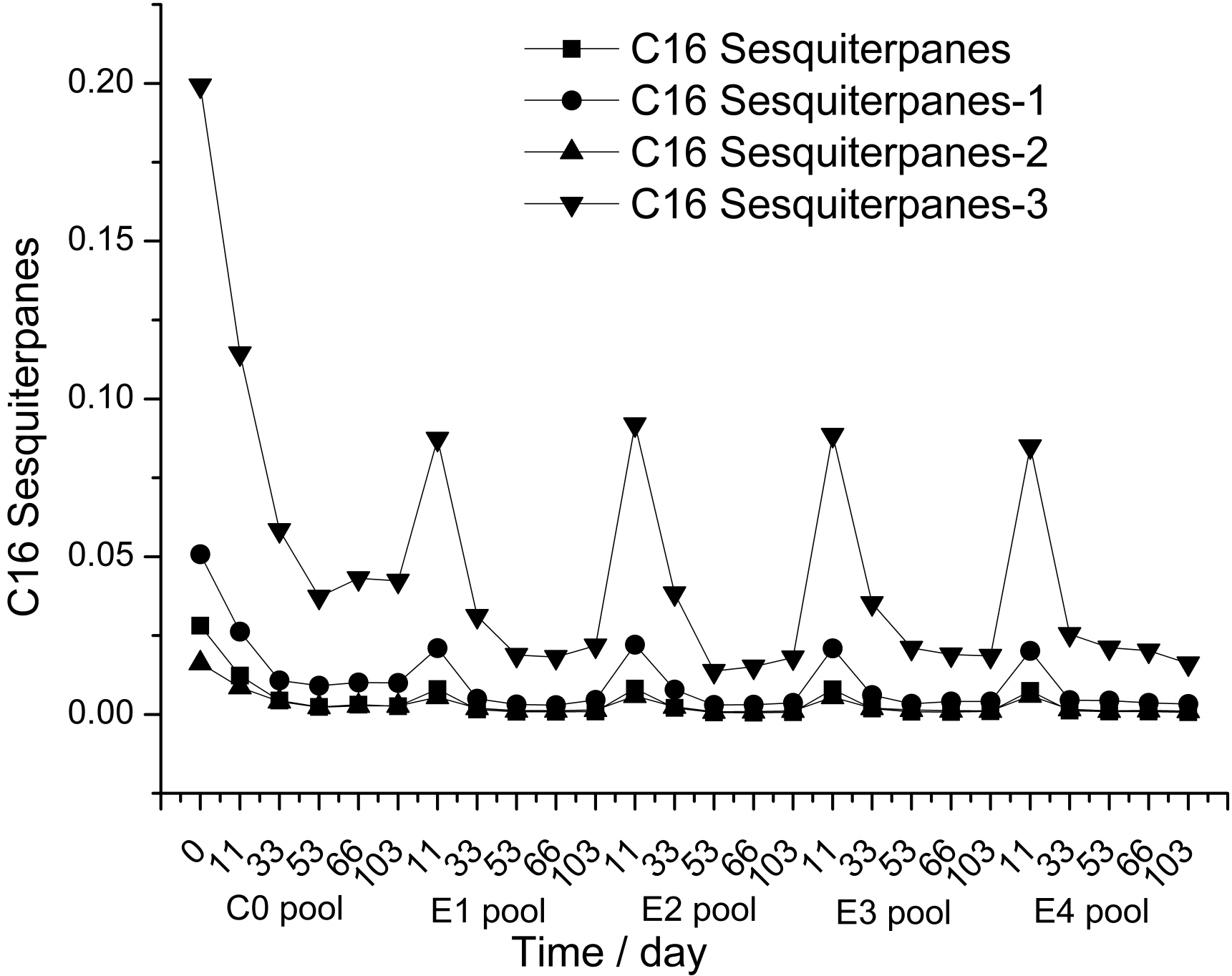

Table 1 The details of biodegradation of crude oil under field simulated conditions

Pool No.	Pool type	Adding materials
B0	blank pool	nothing
C0	control pool	crude oil
E1	experimental pool	crude oil, N1-N4
E2	experimental pool	crude oil, N1-N4, rhamnolipid biosurfactants
E3	experimental pool	crude oil, N1-N4, nutrients
E4	experimental pool	crude oil, N1-N4, rhamnolipid biosurfactants, nutrients

Table 2 Statistic of relative peak area of tricycle diterpanes, hopanes, and steranes normalized to the conservative, nonbiodegradable biomarker C30-17α(H), 21β(H)-hopane) in the control pool C0 and the experimental pools of E1, E2, E3, and E4

	Maximum value	Minimum value	RSD (%)
C21 13b(H),14a(H)-tricycle diterpanes	0.02	0.02	11.06
C22 13b(H),14a(H)-tricycle diterpanes	0.01	0.01	10.53
C23 13b(H),14a(H)-tricycle diterpanes	0.03	0.02	6.27
C24 13b(H),14a(H)-tricycle diterpanes	0.01	0.01	4.21
C25 13b(H),14a(H)-tricycle diterpanes	0.01	0.01	4.03
C26 13b(H),14a(H)-tricycle diterpanes	0.01	0.01	8.93
C26 13b(H),14a(H)-tricycle diterpanes-1	0.03	0.03	3.44
18a(H),21b(H)-22,29,30-(Ts) trisnorhopane	0.16	0.11	9.61
17a(H),21b(H)-22,29,30-(Tm) trisnorhopane	0.09	0.08	1.99
17a(H),21b(H)-30-norhopane +18^{a}(H)-30-trisnorneohopane	0.60	0.56	1.34
17b(H),21a(H)-30-norhopane	0.07	0.06	4.06
17a(H),21b(H)-hopane	1.00	1.00	0.00
17b(H),21a(H)-moretane	0.15	0.12	5.90
22S-17a(H),21b(H)-homohopane	0.35	0.32	1.69
22R-17a(H),21b(H)-homohopane	0.26	0.22	4.45
Gammacerane	0.18	0.11	10.79
22S-17a(H),21b(H)-bishomohopane	0.24	0.22	2.22
22R-17a(H),21b(H)-bishomohopane	0.18	0.17	2.04
22S-17a(H),21b(H)-trishomohopane	0.17	0.15	2.59
22R-17a(H),21b(H)-trishomohopane	0.12	0.11	2.98

22S-17a(H),21b(H)-tetrakishomohopane	0.12	0.10	4.24
22R-17a(H),21b(H)-tetrakishomohopane	0.07	0.06	4.64
22S-17a(H),21b(H)-pentakishomohopane	0.05	0.04	5.58
22R-17a(H),21b(H)-pentakishomohopane	0.05	0.03	13.13
20S-10a(H),13b(H),17a(H)-diacholestane	0.03	0.02	6.02
20R-10a(H),13b(H),17a(H)-diacholestane	0.02	0.02	5.80
20S-5a(H),14a(H),17a(H)-cholestane	0.05	0.04	6.06
20R-5a(H),14b(H),17b(H)-cholestane	0.06	0.05	6.01
20S-5a(H),14b(H),17b(H)-cholestane	0.06	0.04	10.42
20R-5a(H),14a(H),17a(H)-cholestane	0.08	0.06	5.25
20S-5a(H),14a(H),17a(H)-24-methylcholestane	0.04	0.03	6.12
20R-5a(H),14b(H),17b(H)-24-methylcholestane	0.06	0.05	4.48
20S-5a(H),14b(H),17b(H)-24-methylcholestane	0.04	0.03	5.56
20R-5a(H),14a(H),17a(H)-24-methylcholestane	0.06	0.06	2.82
20S-5a(H),14a(H),17a(H)-24-ethylcholestane	0.06	0.05	6.85
20R-5a(H),14b(H),17b(H)-24-ethylcholestane	0.06	0.05	6.06
20S-5a(H),14b(H),17b(H)-24-ethylcholestane	0.04	0.03	7.22
20R-5a(H),14a(H),17a(H)-24-ethylcholestane	0.08	0.07	4.26
Maximum value	1.00	1.00	13.13
Minimum value	0.01	0.01	0.00
average value	0.12	0.11	5.49